Journal of Photochemistry and Photobiology A: Chemistry 200 (2008) 181–186

Contents lists available at ScienceDirect

Journal of Photochemistry and Photobiology A: Chemistry

journal homepage: www.elsevier.com/locate/jphotochem

Multifunctional photo acid generator for fluorescence imaging based on self-contained photoreaction

Takatsugu Endo[a], Shota Suzuki[a], Nobukazu Miyagawa[b], Shigeru Takahara[b,*]

[a] Graduate School of Science and Technology, Chiba University, 1-33 Yayoi-cho, Inage-ku, Chiba 263-8522, Japan
[b] Graduate School of Advanced Integration Science, Chiba University, 1-33 Yayoi-cho, Inage-ku, Chiba 263-8522, Japan

ARTICLE INFO

Article history:
Received 19 January 2008
Received in revised form 11 June 2008
Accepted 10 July 2008
Available online 29 July 2008

Keywords:
Fluorescence imaging
Photoacid generator
Photoinduced electron transfer
Multifunctional material
1,8-Naphthalimide

ABSTRACT

We present *N*-(*p*-anilinesulfonyloxy)-1,8-naphthalimide (ASNI) as fluorescence imaging material based on a novel fluorescence imaging mechanism. ASNI is composed of two functional moieties in one molecule: an acid-reactive fluorescence probe and a photoacid generator (PAG). When ASNI is photoirradiated, a bond in the PAG moiety breaks and an acid is generated. The fluorescence probe moiety then detects the acid and fluoresces. We call this novel mechanism a self-contained photoreaction (SCP). The photophysical properties and photoreactivity of ASNI were measured and compared with those of a prototype PAG, *N*-(phenylsulfonyloxy)-1,8-naphthalimide. These were well represented by density functional theory calculations. SCP permits one-step fluorescence imaging without any wet or dry developing process.

1. Introduction

Fluorescence imaging plays an important role in both fundamental and applied science. Excellent reviews of luminescent sensors, switch molecules corresponding to various targets [1], and fluorescence of polymer films by photomasked irradiation of precursors of fluorescent material [2] have been published. Methods of fluorescence imaging have been widely investigated in biosensor [3–8], chemosensor [9–13], printing [14,15], and other imaging industries.

Typical fluorescence imaging method employs wet developing procedure while such system has some intrinsic problems due to its wet developing procedure, for example, the difficulty of dye penetration into polymer matrices [2]. Therefore, dry developing procedure has been recently investigated. The dry developing imaging system generally includes three components: fluorophore precursor, photoinitiator, and polymer matrix. In many cases photoinitiator is photoacid generator (PAG). Some researchers have reported one or two component imaging systems by conjugation of fluorophore precursor and/or photoinitiator to the polymer matrix [16–23]. These systems have some advantages over the three component systems, e.g., easy preparation, high thermal, and long term stability of imaging film. While the multifunctionalization has been focused on polymer pendant, there are no reports on the fluorophore precursor–photoinitiator conjugated material.

Here we report a fluorophore precursor embedded in photoinitiator for fluorescence imaging with dry developing procedure. This material has some advantages compared to conventional three components materials. First is easy preparation of the imaging film. Second is low exposure energy loss because it is absorbed by the photoinitiator at the initial stage of photoirradiation. Third is providing a novel photoimaging system based on self-contained photoreaction (SCP). Fig. 1 shows general fluorescence imaging mechanism based on photoinduced electron transfer (PET) [24–28]. We introduced a photoacid-generating group as photoinitiator between the fluorophore and the acid receptor in place of the spacer as shown in Fig. 2. Photoexcitation of the fluorophore leads to PET from the receptor to the fluorophore, because the energy level of the receptor is higher than that of the fluorophore. Therefore, the fluorophore cannot emit luminescence before photoirradiation. After photoirradiation, an acid is generated from a photoacid-generating group and combined to the receptor of another molecule. Since the energy level of the receptor combined with the acid is lower than that of the fluorophore, PET does not occur and the fluorescence is observed. It is remarkable that the sequence of giving fluorescence to the initial compound by the acidic product is present in the photoreaction.

* Corresponding author. Tel.: +81 43 290 3461; fax: +81 43 290 3461.
E-mail address: takahara@faculty.chiba-u.jp (S. Takahara).

1010-6030/$ – see front matter © 2008 Elsevier B.V. All rights reserved.
doi:10.1016/j.jphotochem.2008.07.009

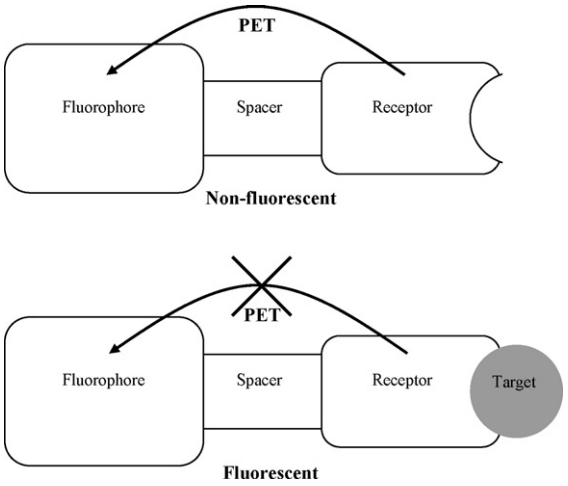

Fig. 1. Mechanism of fluorescence probe based on PET (X = H^+ or metal ion).

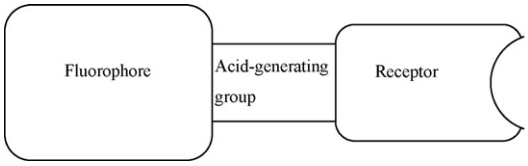

Fig. 2. Illustration of novel fluorescence probe with a photoacid generation function.

2. Experimental

2.1. Materials

Synthetic procedures of the materials used in this report are shown in Scheme 1. To prepare *N*-(*p*-anilinesulfonyloxy)-1,8-naphthalimide (ASNI), we added aniline-4-sulfochloride (8 mmol) [29] to a solution of *N*-hydroxy-1,8-naphthalimide (16 mmol) [30] in dry pyridine (12 ml). The mixture was stirred for 1 h at 115 °C under an argon atmosphere, then it was poured onto excess distilled water and filtered. The product was washed successively with 1N NaOH aq., distilled water, and ethanol. It was purified by silica gel chromatography with pyridine/chloroform (1:4, v/v). Recrystallization of the product from pyridine/toluene (1:1, v/v) gave ASNI (4 mmol, yield 48%). ^{1}H NMR (500 MHz, DMSO-d_6): δ 8.54–8.49 (q, 4H), 7.93–7.90 (t, 2H), 7.63–7.60 (d, 2H), 6.68–6.65 (d, 2H), 6.56 (s, 2H); FT-IR (cm^{-1}, KBr): 1166, 1371 (SO_2 stretching), 1697 (C=O stretching), 3252, 3359, 3459 (NH_2 stretching). *N*-(Phenylsulfonyloxy)-1,8-naphthalimide (PSNI) was prepared as described [30,31] for comparison of its photophysical properties and photoreactivity with those of ASNI.

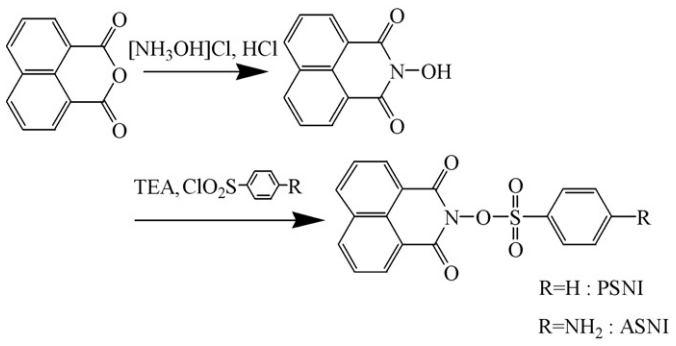

Scheme 1. Procedures for synthesis of ASNI and PSNI.

2.2. Apparatus and measurements

Nuclear magnetic resonance (NMR) spectra were obtained with a JEOL LA-500 spectrometer with tetramethylsilane as an internal standard. Fourier transform infrared (FT-IR) spectra were recorded on a Horiba FT-200 spectrometer. Absorption spectra and fluorescence spectra excited at 315 nm were measured with a Hitachi U-3000 spectrophotometer and a Hitachi F-4500 spectrophotometer, respectively.

All samples in acetonitrile solutions were degassed by Ar bubbling for at least 15 min, then absorption and fluorescence spectra of the solutions were measured. Fluorescence quantum yields (ϕ_f) were obtained as described [32] using anthracene in ethanol as a standard. Acid generation quantum yields (ϕ_{acid}) were determined as described [33] with a low-pressure mercury lamp (254 nm, 0.4 mJ cm^{-2} s^{-1}), using the sodium salt of tetrabromophenol blue (TBPB-Na, Sigma–Aldrich) as an acid indicator and *p*-toluenensulfonic acid (Wako) as a standard.

To obtain a photosensitive polymer film, we prepared a 20 wt% solution of poly(methylmethacrylate) (Wako, DLH6175) in *N*,*N*-dimethylformamide, then dissolved 2 wt% ASNI in it. The mixture was spin-coated onto a glass plate at 2000 rpm for 1 min, then the plate was baked at 100 °C for 10 min.

2.3. Density functional theory calculations

Density functional theory (DFT) calculations were performed using the Gaussian 03 program package [34]. Structure geometries were optimized at the B3LYP/6-31G(d) level, and time-dependent (TD) DFT calculations were carried out at the B3LYP/6-311++G(d,p) level.

3. Results and discussion

3.1. Photophysical properties

Fig. 3 shows absorption and fluorescence spectra of ASNI and PSNI in acetonitrile. Table 1 summarizes the photophysical properties. The absorption bands between 310 and 360 nm are associated with the naphthalimide moiety, because λ_{max} of 1,8-naphthalimide in acetonitrile is 328 nm [35]. The two absorption spectra differed greatly in the region from 250 to 310 nm. ASNI had a strong absorption peak at 284 nm, which PSNI lacked. Since the λ_{max} of aniline is around 280 nm, the absorption is likely due to the aniline group in ASNI.

The fluorescence spectra presented an interesting result (Fig. 3B). We select naphthalimide moiety as fluorophore because its derivatives are well-known as high fluorescent materials [36–38]. The PSNI fluorescence (ϕ_f = 0.201) was stronger than that of 1,8-naphthalimide (ϕ_f = 0.03 [39]): ASNI showed very weak fluorescence in spite of its fluorophore. According to previous reports

Table 1
Photophysical properties of ASNI and PSNI

	ASNI	PSNI
λ_{max} (nm)	214, 231, 284, 333	230, 334
ε_{284} (M^{-1} cm^{-1})	22,900	1830
E_{max} (nm)	366, 382	366, 381
ϕ_f	<0.001	0.201

λ_{max}: maximum absorption wavelengths, ε_{284}: molecular extinction coefficient at 284 nm, E_{max}: maximum fluorescence wavelengths.

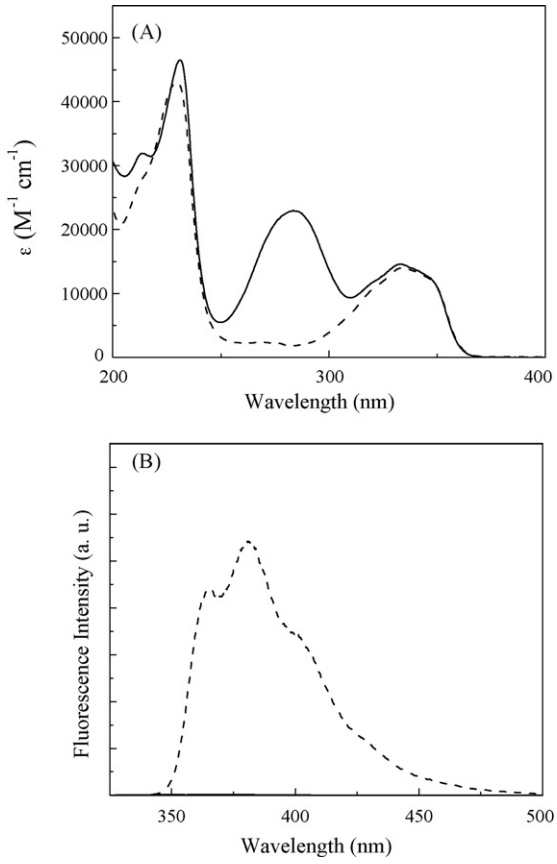

Fig. 3. (A) Absorption and (B) fluorescence spectra of ASNI (solid line) and PSNI (dashed line).

[24–28], the fluorescence is quenched by PET in an excited ASNI molecule, as illustrated in Fig. 1.

We used DFT calculations to understand the unusual photophysical properties of ASNI. DFT calculations are effective for the rational design of PET-based fluorescence probes [27,28]. The excitation spectra of ASNI and protonated ASNI (ASNI-H^+) were calculated by the TD-DFT method and are shown in Fig. 4. Both compounds have a strong absorption peak around 340 nm, in agreement with the experimental results. We attribute these absorptions to the electronic transitions between molecular orbitals associated with the

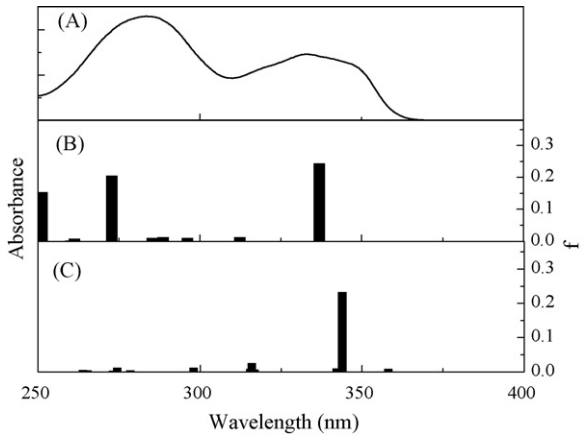

Fig. 4. (A) Observed absorption spectrum of ASNI and (B) calculated absorption spectra of ASNI, and (C) ASNI-H^+ estimated by TD-DFT.

naphthalimide fluorophore. The calculated absorption at 273 nm is present only in ASNI, and agrees with the observed result. The absorption is due to the transition contributed from the aniline moiety estimated by the calculation. We attribute the disappearance of the absorption around 280 nm in ASNI-H^+ to protonation of the aniline group in ASNI.

We calculated the frontier molecular orbitals of ASNI and ASNI-H^+ to examine the fluorescence switching mechanism (Fig. 5). The calculation represented the mechanism well, as did previous results with perylene compounds [27]. In ASNI (Fig. 5A), the highest occupied molecular orbital (HOMO), distributed mainly on the fluorophore (HOMO-2), has lower energy than that on the receptor (HOMO-0, HOMO-1). Therefore, when the fluorophore is excited, an electron on HOMO-0 or HOMO-1 transfers to HOMO-2 in the molecule. In this case, PET prevents fluorescence from the naphthalimide moiety. In ASNI-H^+, HOMO, again distributed mainly on the fluorophore, has higher energy than that on the receptor (Fig. 5B). Since electron transfer from the receptor to the fluorophore does not occur, fluorescence is observed, because the process does not compete with PET. These results suggest that ASNI could work as a fluorescence probe for acids.

3.2. Behavior of ASNI as proton-target fluorescence probe

We measured the fluorescence of ASNI in acetonitrile solution with various concentrations of *p*-toluenesulfonic acid to evaluate

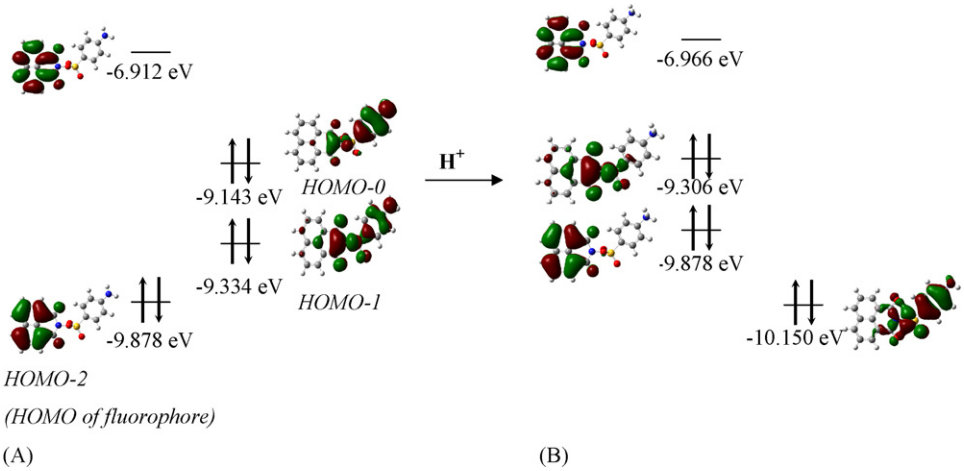

Fig. 5. Frontier molecular orbitals of (A) ASNI and (B) ASNI-H^+.

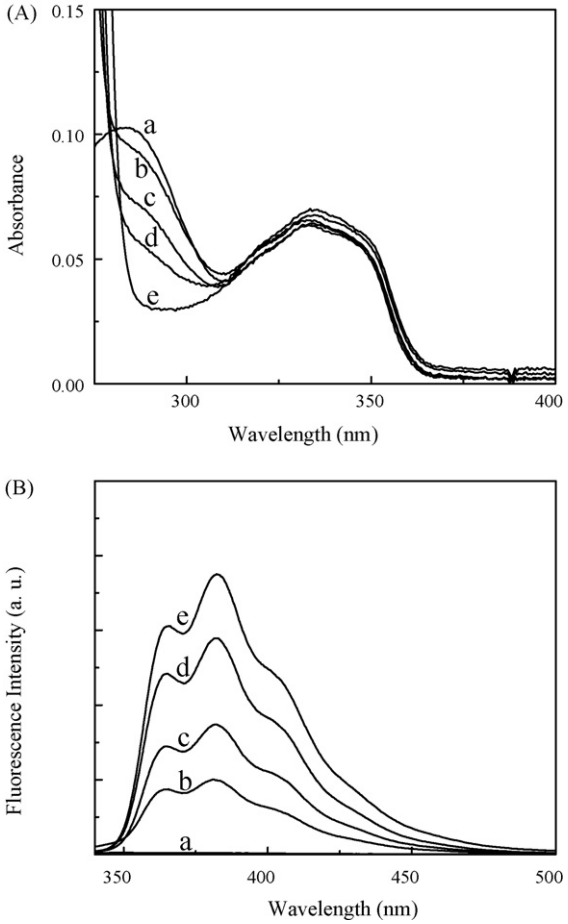

Fig. 6. (A) Absorption and (B) fluorescence spectra of ASNI in acetonitrile (4.33 μmol l^{-1}) with various concentrations of *p*-toluenesulfonic acid ((a) 0.0 mmol l^{-1}, (b) 0.9 mmol l^{-1}, (c) 1.7 mmol l^{-1}, (d) 3.5 mmol l^{-1}, and (e) 13.6 mmol l^{-1}).

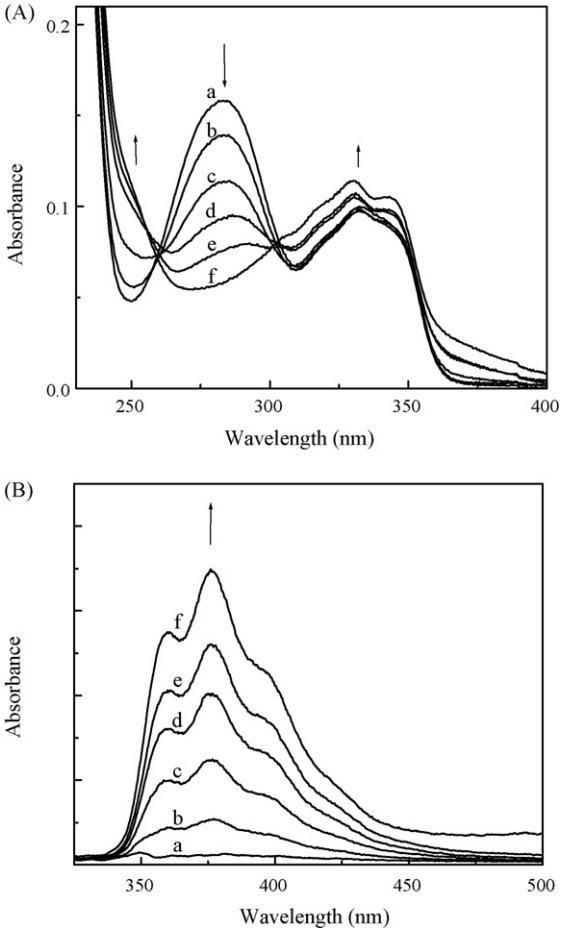

Fig. 7. (A) Absorption and (B) fluorescence spectra of ASNI in acetonitrile (6.85 μmol l^{-1}) under irradiation ((a) 0.000 J cm^{-2}, (b) 0.264 J cm^{-2}, (c) 0.792 J cm^{-2}, (d) 1.584 J cm^{-2}, (e) 2.376 J cm^{-2}, and (f) 5.940 J cm^{-2}).

ASNI as a fluorescent probe for acids. The changes in the absorption and fluorescence spectra of the ASNI solution caused by the addition of the acid are shown in Fig. 6A and B, respectively. Despite the decrease of the absorption at 284 nm, the fluorescence intensity increased with the increasing concentration of acid. The highest ϕ_f value of ASNI-H$^+$ (0.149) was more than 100 times that of ASNI (<0.001), and approximately the same as that of PSNI (0.201).

These spectrum changes are well explained by the results of the molecular orbital calculations. The diminution of the ASNI absorption peak at 284 nm which originated from the aniline group indicates the protonation of the aniline group and the formation of ASNI-H$^+$. Fluorescence occurs because the HOMO of the protonated receptor becomes lower in energy than that of the fluorophore. This prohibits intramolecular PET in ASNI-H$^+$.

3.3. Photoreaction of ASNI

We compared the photoreactivity of ASNI with that of PSNI under photoirradiation. Values of ϕ_{acid} were 0.071 for ASNI and 0.037 for PSNI. The ASNI value is higher, although the amino group of ASNI should decrease it. Although ϕ_{acid} depends on several factors, the simplest explanation for the higher ϕ_{acid} value would be the difference in the bond dissociation energy (BDE) of N–O cleavage. We calculated the BDEs of N–O cleavage of the two PAGs by using DFT at the B3LYP/6–31G(d) level. Because *N*-tosyloxy-1,8-naphthalimide, an analogue of ASNI and PSNI, generates acid through homolytic cleavage [40], we assumed the same process in our calculations. We corrected for the consequent superposition error [41] by using the counterpoise method [42]. The BDEs of N–O cleavage of ASNI and PSNI were estimated to be 215.6 and 227.6 kJ mol^{-1}, respectively, and showed a good correlation with ϕ_{acid}. Such a relation was found in substituted anilines [43], but not in some photoradical generators [44]. If ϕ_{acid} also depends on whether photodissociation is due to homolytic or heterolytic cleavage [40], then we cannot conclude the reason for the higher ϕ_{acid} of ASNI from our results. However, introducing an amino group to a PAG is one of the reasons for a high ϕ_{acid}.

Fig. 7 shows absorption and fluorescence spectra of ASNI in acetonitrile under irradiation. The absorption spectrum decreased and the fluorescence spectrum increased with increasing exposure energy, as seen with the addition of acid to ASNI in Fig. 6. From this result, we propose a novel imaging system based on the SCP mechanism using ASNI as shown in Scheme 2. ASNI is a non-fluorescent molecule because of intramolecular PET. Once ASNI is excited by photoirradiation, sulfanilic acid is generated through N–O bond cleavage. This acid binds to an amino group of unphotoreacted ASNI. This protonated ASNI, ASNI-H$^+$, fluoresces because intramolecular PET does not occur. Since both steps occur in the same molecule, we call the reaction a self-contained photoreaction.

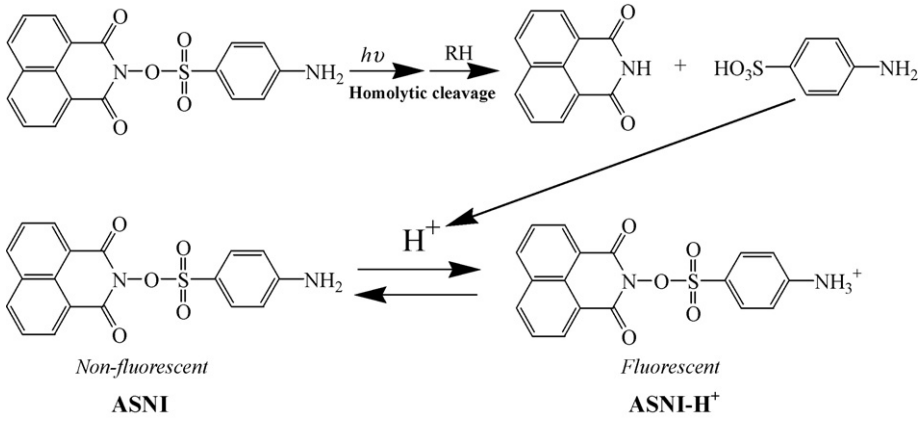

Scheme 2. Self-contained photoreaction of ASNI (RH: hydrogen donor).

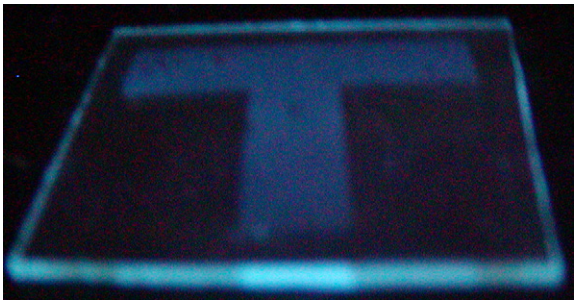

Fig. 8. Fluorescence image made by UV-irradiation through a T-shape mask.

3.4. Imaging in polymer film

Finally, we demonstrated SCP in one-step fluorescence imaging. The plate was irradiated with a low-pressure mercury lamp ($4\,J\,cm^{-2}$) through a T-shape mask. Fig. 8 shows a fluorescent image under UV illumination without any wet or dry developing process, indicating the occurrence of SCP in the polymer film.

4. Conclusion

We have designed and synthesized a multifunctional molecule, ASNI. The photophysical properties of ASNI are significantly different from those of PSNI. Unlike PSNI, ASNI has an absorption peak at 284 nm and shows very weak fluorescence. The differences are well explained by DFT calculations. The photoreactivity of ASNI and the spectral changes in fluorescence caused by the addition of an acid indicate that ASNI acted as both a fluorescent probe for the acid and a PAG. SCP occurs in ASNI, allowing one-step fluorescence imaging in a polymer matrix of ASNI without any wet or dry developing process.

Although we have provided novel photoimaging material and imaging system, there are some challenging tasks on the material, especially photosensitivity. Study to perform the task is currently underway in our laboratory.

Acknowledgment

We thank the Institute of Media and Information Technology of Chiba University for the facilities and the use of the Hitachi SR11000/J1.

References

[1] J.F. Callan, A.P. de Silva, D.C. Magri, Tetrahedron 61 (2005) 8551.
[2] J.-M. Kim, Macromol. Rapid Commun. 28 (2007) 1191.
[3] G. Grynkiewicz, M. Poenie, R.Y. Tsien, J. Biol. Chem. 260 (1985) 3440.
[4] Y. Suzuki, K. Yokoyama, J. Am. Chem. Soc. 127 (2005) 17799.
[5] H. Komatsu, T. Miki, D. Citterio, T. Kubota, Y. Shindo, Y. Kitamura, K. Oka, K. Suzuki, J. Am. Chem. Soc. 127 (2005) 10798.
[6] S. Weiss, Science 283 (1999) 1676.
[7] K. Kawai, K. Kawabata, S. Tojo, T. Majima, Bioorg. Med. Chem. Lett. 12 (2002) 2363.
[8] G. Seisenberger, M.U. Ried, T. Endreß, H. Büning, M. Hallek, C. Bräuchle, Science 294 (2001) 1929.
[9] Z. Xu, X. Qian, J. Cui, Org. Lett. 7 (2005) 3029.
[10] S. Brasselet, W.E. Moerner, Single Mol. 1 (2000) 17.
[11] M.D. Mason, K. Ray, G. Pohlers, J.F. Cameron, R.D. Grober, J. Phys. Chem. B 107 (2003) 14219.
[12] Y. Hou, A.M. Bardo, C. Martinez, D.A. Higgins, J. Phys. Chem. B 104 (2000) 212.
[13] J.C. Scaiano, M. Laferriere, M.G. Ivan, Macromolecules 36 (2003) 6692.
[14] S. Natarajan, S.H. Kim, Langmuir 21 (2005) 7052.
[15] B.A. Langowski, K.E. Uhrich, Langmuir 21 (2005) 10509.
[16] J.-H. Lee, I. Cho, K.-D. Ahn, J.-M. Kim, Chem. Lett. 30 (2001) 716.
[17] J.-M. Kim, T.-E. Chang, J.-H. Kang, K.H. Park, D.-K. Han, K.-D. Ahn, Angew. Chem. Int. Ed. 39 (2000) 1780.
[18] C.-W. Lee, Z. Yuan, K.-D. Ahn, S.-H. Lee, Chem. Mater. 14 (2002) 4572.
[19] J.-M. Kim, T.-E. Chang, J.-H. Kang, D.K. Han, K.-D. Ahn, Adv. Mater. 11 (1999) 1499.
[20] H. Tian, J. Gan, K. Chen, J. He, Q.L. Song, X.Y. Hou, J. Mater. Chem. 12 (2002) 1262.
[21] J. Yoo, J.-H. Lee, I. Cho, K.-D. Ahn, J.-M. Kim, Macromol. Res. 11 (2003) 69.
[22] J.-H. Yoo, S.-Y. Kim, I. Cho, J.-M. Kim, K.-D. Ahn, J.-H. Lee, Polymer 45 (2004) 5391.
[23] J. Gan, H. Tian, K. Chen, Polym. Adv. Technol. 13 (2002) 584.
[24] A.P. de Silva, D.B. Fox, A.J.M. Huxley, T.S. Moody, Coord. Chem. Rev. 205 (2000) 41.
[25] L. Zang, R. Liu, M.W. Holman, K.T. Nguyen, D.M. Adams, J. Am. Chem. Soc. 124 (2002) 10640.
[26] S. Abad, M. Kluciar, M.A. Miranda, U. Pischel, J. Org. Chem. 70 (2005) 10565.
[27] P. Yan, M.W. Holman, P. Robustelli, A. Chowdhury, F.I. Ishak, D.M. Adams, J. Phys. Chem. B 109 (2005) 130.
[28] K. Tanaka, T. Miura, N. Umezawa, Y. Urano, K. Kikuchi, T. Higuchi, T. Nagano, J. Am. Chem. Soc. 123 (2001) 2530.
[29] J. Contreras, J.I. Jones, Br. Polym. J. 12 (1980) 192.
[30] C. Iwashima, G. Imai, H. Okamura, M. Tsunooka, M. Shirai, J. Photopolym. Sci. Technol. 16 (2003) 91.
[31] H.W. Altoland, R.W. Ryan Jr., Japan Patent 190,947 (1983).
[32] B. Valeur, Molecular Fluorescence, Wiley-VCH, New York, 2001, pp. 159–161.
[33] M. Shah, N.S. Allen, N.G. Salleh, T. Corrales, M. Egde, F. Catalina, P. Bosch, A. Green, J. Photochem. Photobiol. A: Chem. 111 (1997) 229.
[34] M.J. Frisch, G.W. Trucks, H.B. Schlegel, G.E. Scuseria, M.A. Robb, J.R. Cheeseman, J.A. Montgomery Jr., T. Vreven, K.N. Kudin, J.C. Burant, J.M. Millam, S.S. Iyengar, J. Tomasi, V. Barone, B. Mennucci, M. Cossi, G. Scalmani, N. Rega, G.A. Petersson, H. Nakatsuji, M. Hada, M. Ehara, K. Toyota, R. Fukuda, J. Hasegawa, M. Ishida, T. Nakajima, Y. Honda, O. Kitao, H. Nakai, M. Klene, X. Li, J.E. Knox, H.P. Hratchian, J.B. Cross, C. Adamo, J. Jaramillo, R. Gomperts, R.E. Stratmann, O. Yazyev, A.J. Austin, R. Cammi, C. Pomelli, J.W. Ochterski, P.Y. Ayala, K. Morokuma, G.A. Voth, P. Salvador, J.J. Dannenberg, V.G. Zakrzewski, S. Dapprich, A.D. Daniels, M.C. Strain, O. Farkas, D.K. Malick, A.D. Rabuck, K. Raghavachari, J.B. Foresman, J.V. Ortiz, Q. Cui, A.G. Baboul, S. Clifford, J. Cioslowski, B.B. Stefanov, G. Liu, A. Liashenko, P. Piskorz, I. Komaromi, R.L. Martin, D.J. Fox, T. Keith, M.A. Al-Laham,

C.Y. Peng, A. Nanayakkara, M. Challacombe, P.M.W. Gill, B. Johnson, W. Chen, M.W. Wong, C. Gonzalez, J.A. Pople, Gaussian 03, Gaussian, Inc., Wallingford, CT, 2004.
[35] E. Martin, J.L.Gu. Coronado, J.J. Camacho, A. Pardo, J. Photochem. Photobiol. A: Chem. 175 (2005) 1.
[36] I. Grabchev, J.-M. Chovelon, X. Qian, J. Photochem. Photobiol. A: Chem. 158 (2003) 37.
[37] J. Li, F. Meng, H. Tian, J. Mi, W. Ji, Chem. Lett. 34 (2005) 922.
[38] T.C. Barros, G.R. Molinari, P.B. Filho, V.G. Toscano, M.J. Politi, J. Photochem. Photobiol. A: Chem. 76 (1993) 55.
[39] V. Wintgens, P. Valat, J. Kossanyi, L. Biczok, A. Demeter, T. Bérces, J. Chem. Soc., Faraday Trans. 90 (1994) 411.
[40] F. Ortica, J.C. Scaiano, G. Pohlers, J.F. Cameron, A. Zampini, Chem. Mater. 12 (2000) 414.
[41] B.J. Ransil, J. Chem. Phys. 34 (1961) 2109.
[42] S.F. Boys, F. Bernardi, Mol. Phys. 19 (1970) 553.
[43] M.F. Budyka, T.S. Zyubina, A.K. Zarkadis, J. Mol. Struct. (Theochem) 594 (2002) 113.
[44] X. Allonas, J. Lalevée, J.P. Fouassier, J. Photochem. Photobiol. A: Chem. 159 (2003) 127.